Title: Estimation of ‘Hass’ avocado (*Persea americana* Mill.) ripeness by fluorescence fingerprint measurement

Authors: Mito Kokawa[a*], Azusa Hashimoto[b], Xinyue Li[c], Mizuki Tsuta[c], Yutaka Kitamura[a]

Affiliations:

a) Faculty of Life and Environmental Sciences, University of Tsukuba, 1-1-1 Tennodai, Tsukuba, 305-8572 Ibaraki, Japan

b) School of Life and Environmental Sciences, University of Tsukuba, 1-1-1 Tennodai, Tsukuba, 305-8572 Ibaraki, Japan

c) National Agriculture and Food Research Association, Food Research Institute, 2-1-12 Kannondai, Tsukuba, 305-8642 Ibaraki, Japan

Corresponding author:

Mito Kokawa

kokawa.mito.ke@u.tsukuba.ac.jp

Tel: +81-29-853-4659

Fax: +81-29-853-4659

Abstract

Avocados (*Persea americana* Mill.) are a climacteric fruit which ripen until after harvesting, and their ripeness is an important quality attribute that determines consumer liking. In this study, the ripening degree of 'Hass' avocados was evaluated non-destructively by measuring the skin and flesh using the fluorescence fingerprint (FF). FF, also known as the Excitation emission matrix (EEM), is a set of fluorescence spectra obtained at consecutive excitation wavelengths. It was found that as ripening progressed, the fluorescence signal of chlorophyll A in the skin and flesh decreased significantly as the hardness of the avocado flesh decreased. The hardness value was estimated from the FFs of the skin and flesh using partial least-squares regression, and minimum prediction errors of 2.02 N cm^{-2} and 2.05 N cm^{-2} were obtained for the prediction models using FFs of the flesh and skin, respectively. Furthermore, ripeness levels (unripe, ripe, and over ripe) were discriminated non-destructively from the FFs of the skin with an accuracy of 90% for the validation dataset. The measurement and analysis technique demonstrated in this study is rapid and accurate, and can contribute to supplying uniform agricultural products to consumers.

Keywords:

Excitation emission matrix (EEM); Partial least-squares regression; discrimination analysis; texture measurement; polyphenol oxidase

Introduction

Avocados (*Persea americana* Mill.) are a climacteric fruit that ripens after harvesting. Maturation of the fruit occurs while the fruit is on the tree, and maturation is characterized by an increase in the fat content and a concurrent decrease in the water content (Clark et al. 2007). Interestingly, the avocado fruit does not ripen while it is on the tree and remains green and hard (Paliyath et al. 2008). After harvesting, ripening occurs, characterized by a change in color (green to black or purple, especially for the 'Hass' variety) and softening of the flesh.

Although there have been many reports on predicting the maturity of avocado fruit non-destructively, as reviewed by Magwaza and Tesfay (2015), there have been fewer reports on monitoring avocado ripeness after their harvest. Gaete-Garretón et al. (2005) applied ultrasonic methods to assess avocado ripeness and showed that the adsorption coefficient had a strong correlation with firmness, but this correlation was only obtained from the average values of 15 fruit. Cox et al. (2004) showed that the avocado skin color changes during ripening owing to a decrease in chlorophyll and an increase in anthocyanins, more specifically, cyanidin-3-gluocoside. Color changes in the skin are

also an important indicator of ripeness for consumers (Pareek 2016) especially for varieties such as ‘Hass’, but there has been no work using vibrational spectroscopic techniques to accurately evaluate the ripening degree of avocados. However, evaluating the ripening degree of avocados quickly and accurately is important for providing uniform fruit to consumers, especially to the catering industry, where certain amounts of ready-to-eat fruit are needed daily.

The skin and flesh of avocados contain multiple fluorescent compounds, including chlorophyll, tocopherols and many polyphenols such as chlorogenic, cinnamic, and caffeic acid (Rodriguez-Carpena et al. 2011; Schroeder 1987). During ripening, the chlorophyll content in the skin (Cox et al. 2004) and flavonoids such as epicatechins (George and Christoffersen 2016) decrease. Therefore, fluorescence measurement is potentially effective for measuring the degree of ripeness of avocados.

Rather than directly targeting the fluorophores mentioned above and acquiring single fluorescence spectra to measure each compound, this study uses the fluorescence fingerprint (FF), also known as the excitation-emission matrix (EEM), to acquire more comprehensive information about the fruit. FFs are a set of fluorescence spectra acquired

at consecutive excitation wavelengths (Jiang et al. 2010), giving a three-dimensional diagram consisting of fluorescence intensity values at different excitation and emission wavelengths. The advantage of the FF technique over conventional fluorescence spectroscopy is that it includes the signals of many fluorescent constituents existing in the sample. Therefore, simultaneous changes in multiple constituents can be measured at once. Many studies using the FF technique to measure various food stuffs such as ham (Moller et al. 2003), olive oil (Guimet et al. 2004), beer (Sikorska et al. 2008), cheese (Kokawa et al. 2015), soymilk (Kokawa et al. 2016), and peaches (Trivittayasil et al. 2017) have been reported.

This study aims to use the FF technique to estimate the degree of ripeness of avocados non-destructively by measuring the fluorescence of the skin and flesh. Measurement of the skin can be performed non-destructively and is applicable for product monitoring, while measurement of the flesh enabled us to acquire comprehensive information about the chemical changes occurring in avocados during ripening.

Materials and methods

1. Materials

Sixty avocados of the 'Hass' variety (geographical origin: Mexico) were acquired from Kasumi Co., Ltd. (Ibaraki, Japan) randomly at different purchase times, while they were still unripe. The fruits were stored at refrigeration temperatures during transport. After acquisition, they were transferred to a temperature-controlled room (21 ˚C) and stored until measurement.

2. Evaluation of flesh hardness and ripeness degree

Flesh hardness was measured as an index of ripeness, following the method of Landahl et al. (2009) with some modifications. A texture analyzer (EZ-SX, Shimadzu Corporation, Kyoto, Japan) was used for the hardness measurement. Three cuboid samples of 2.5 cm width and length and 1 cm thickness were cut out from the flesh of each avocado, with the skin removed. A cylindrical plunger with a diameter of 2.0 cm was used to compress the sample for 1.0 mm at a speed of 10 mm min^{-1}, and the maximum stress (N cm^{-2}) was recorded as the hardness of the avocado. The average value of three measurements was used as the hardness value. The hardness measurements of the avocados were performed

on the same day as the FF measurement explained in the next section.

The ripeness degree (‘unripe’, ‘ripe’, and ‘overripe’) of the avocados were determined based on their hardness value as shown in Table 1. The correspondence between ripeness degree and hardness values was determined from pre-experiments using 20 avocados acquired independently from the 60 fruits used in the main experiment.

3. Fluorescence fingerprint measurement

FF measurement of the avocado skin and flesh was performed with a fluorescence spectrophotometer (FP-8500WRE, JASCO, Japan). The samples were measured on an epi-fluorescence platform (EFA-833, JASCO, Japan), where the samples could be pressed upon a flat window of 10 mm diameter. This platform made it possible to measure the avocados without cutting out small samples, thereby leaving the fruit intact for hardness measurement. The excitation and emission wavelength ranges were set to 200–850 nm and 230–850 nm, respectively, and were measured at 10 nm intervals at a speed of 60000 nm min^{-1}. The slit widths of the monochromator used for the excitation and emission lights were both set to 10 nm. The photomultiplier voltage was set at 350 V when

measuring the skin and 270 V when measuring the flesh. After two points on the skin (one near the equatorial plane and one near the basal end) were measured, the avocado was cut in half, and two points of the flesh (one point near the skin and the other near the seed) were measured. The two points on both the skin and flesh were measured to take the heterogeneity within the fruit into account, and the flesh was measured to clarify the chemical changes occurring in the fruit during ripening.

4. Prediction of flesh hardness from FF measurements

A partial least-squares (PLS) regression model was constructed to predict the avocado flesh hardness from the FF data of the skin and flesh. The model was constructed using PLS Toolbox version 8.5.1 (Eigenvector Inc., USA) in MATLAB (R2017b) software (MathWorks Inc., USA).

The FF data were preprocessed before PLS analysis, following the procedure of Kokawa et al. (2015). First, data whose excitation wavelengths were longer than the emission wavelengths were removed. This is because fluorescence has a longer emission wavelength than the excitation wavelength owing to the loss of energy between the

absorption and the fluorescence emission. Next, the first-, second-, and third-order scatter light that occurred at emission wavelengths equal to, twice, and three times the excitation wavelength, respectively, were removed (Fujita et al. 2010). The appearance of the second- and third-order scattered light is due to the light dispersion mechanism of the monochromator. The remaining data, consisting of 1790 combinations of excitation and emission wavelengths, were unfolded (Guimet et al. 2004) into a two-dimensional matrix whose rows represent samples and columns represent wavelength combinations.

The samples were divided into calibration and validation datasets. The fluorescence data from 40 avocados (80 measurements on the skin and 80 measurements on the flesh) were used for calibration, while those from 20 avocados (40 measurements on the skin and 40 measurements on the flesh) were used for validation.

Three preprocessing methods were used for the FF data: mean centering, normalization followed by mean centering, and autoscaling. These were combined with two preprocessing methods for hardness; as is or converted to a log scale. Hardness values were converted to a log scale because the change in fluorescence intensity at some wavelengths was observed to be logarithmically correlated to hardness (details given in

the discussion section). The data were normalized so that the area underneath each spectrum was equal to one. In autoscaling, each wavelength was scaled to zero mean and unit variance.

The number of latent variables for the PLS models was determined by cross-validation with the calibration samples using the Venetian blinds method, where the data is split into groups of s samples, and each test set is determined by selecting every s^{th} object in the group, starting at objects numbered 1 through s ($s = 8$) (Lenhardt et al. 2015). Prediction models formulated using different preprocessing methods were compared based on the root-mean-square error of cross-validation (RMSECV).

5. Discrimination analysis from FF measurements

Avocado ripeness levels (unripe, ripe, and overripe, based on their hardness, Table 1) were predicted by Partial Least-Squares Discrimination Analysis (PLS-DA). Only the FFs of the skin were used for this analysis, assuming practical use where measurement would be done non-destructively without cutting the fruit open. The procedures of FF data preprocessing and construction of the models were similar to those of PLS regression,

except that the three ripeness levels were used as the objective variables. The same three preprocessing methods, mean centering, normalization followed by mean centering, and autoscaling were used to preprocess the FF data.

Results

1. Flesh hardness

The hardness values of the avocados measured in this experiment ranged between 0.52 and 26.7 N cm^{-2}.

2. FFs of avocado skin and flesh

Figure 1 shows the average FFs of the skin and flesh of the unripe, ripe, and overripe avocados. The most prominent fluorescence peak in the FFs of the skin (Fig. 1 top row) can be attributed to chlorophyll A, which fluoresces at emission wavelengths (Em) of approximately 660-680 and 720-740 nm (Schulman 1985). The fluorescence intensity of chlorophyll clearly decreases as ripening progresses. Another fluorescence peak with peak excitation wavelengths (Ex) of 370 nm and Em 450 nm can be observed in the FFs

of the skin. This may be attributed to cinnamic acids such as chlorogenic acid and caffeic acid, which fluoresce around emission wavelengths of 450 nm (Belay et al. 2016; Lang et al. 1991).

The FFs of the avocado flesh (Fig. 1 bottom row) also exhibit chlorophyll fluorescence, but there is a more prominent fluorescence signal at Ex 280 nm and Em 350 nm and a weaker signal at Ex 320 nm and Em 440 nm. This pair of fluorescence peaks is also observed in the FFs of tomatoes (Trivittayasil et al. 2015). Many chemical components emit fluorescence in this wavelength region including tryptophan, tocopherols, and several polyphenols such as epicatechin.

3. Estimation of avocado flesh hardness by PLS regression analysis

Table 2 shows the results of the PLS regression analysis with different preprocessing methods. Estimation accuracy can be evaluated by the root-mean-square error of the calibration (RMSEC), cross-validation (RMSECV), and prediction (RMSEP), and the coefficients of determination of calibration (R^2C), cross-validation (R^2CV), and prediction (R^2P). Models with a small error and a high coefficient of determination of

prediction (RMSEP and R^2P) are accurate. The ratio of the standard deviation of the objective variable (hardness) to RMSEP, known as the residual predictive deviation (RPD) (Lucas et al. 2008; Williams and Sobering 1993), is also shown as a measure of the predictive power of the model. Saeys et al. (2005) stated that models with values of RPD between 1.5 and 2.0 reveal the possibility of differentiating the variability of the data, while values of RPD greater than 2.0 indicate a better predictive performance of the model.

In general, FFs of the flesh showed better performance in predicting avocado hardness than those of the skin. The best model was obtained when the FFs of the flesh were combined with preprocessing by normalization followed by mean centering. The RMSEP of this model was 3.57, indicating that the hardness could be predicted with an average error of 3.57 N cm^{-2}.

Figure 2 shows the regression plots and the variance of importance (VIP) plots of three models that performed well. VIP values summarize the importance of each variable in the model, and because the average VIP value of all the variables equals one, a VIP value greater than one indicates that the variable contributes positively to the model (Chong

and Jun 2005).

Figures 2(a) and 2(d) show the regression and VIP plots of the model using the FFs of the flesh coupled with preprocessing by normalization followed by mean centering. The values predicted from the FFs are generally in accord with those measured with the texture analyzer; however, there are some samples with large errors having hardness values around 12 N cm^{-2}, and some soft samples are predicted to have negative hardness values. The VIP plot of this model shows a prominent peak with excitation and emission wavelengths of 290 and 330 nm, and a smaller peak with excitation and emission wavelengths of 320 and 450 nm, respectively. Furthermore, there is a weak peak corresponding to the wavelengths of chlorophyll A.

To increase estimation accuracy for avocados with moderate hardness, data from avocado fruit whose hardness was above 15 N cm^{-2} were removed from the model because these avocados were clearly distinguishable as unripe by their bright green skin. When models were constructed with the samples softer than 15 N cm^{-2}, RMSE improved considerably as shown in the bottom half of Table 2. The model constructed from the FFs of the skin performed well when preprocessing by autoscaling was used, showing RMSEP

of 2.05 and R^2P of 0.75. Autoscaling worked well for FFs of the flesh, where RMSEP was 2.02 and R^2P was 0.75. RPD increased only slightly because the decrease in RMSEP was canceled out by the limited range of hardness values.

The regression plot for the model constructed from the FFs of the flesh preprocessed by autoscaling is shown in Fig. 2(b). Compared to the model constructed from all the samples, the prediction error for samples with small hardness values decreased considerably, and there were no samples with negative predicted values. Variables with VIP values over 1 (Fig. 2(e)) mainly existed around short excitation wavelengths of 200-300 nm and emission wavelengths of 250-350 nm; around Ex 320 nm and Em 330 nm; and around the wavelengths corresponding to chlorophyll A. The area in the left top corner where the emission wavelength is longer than twice the excitation wavelength may indicate secondary fluorescence, which appears at twice the emission wavelength of its original signal, similarly to secondary scattered light.

Figures 2(c) and 2(f) show the regression and VIP plots of the model constructed from FFs of the skin, preprocessed with autoscaling. The prominent peak in the VIP plot is around Ex 540 nm and Em 780 nm. In contrast to the models using FFs of the flesh, there

are no important variables in the short-wavelength region.

4. Prediction of ripeness levels by PLS discrimination analysis

Table 3 shows the results for the PLS discrimination analysis (validation data) using the FFs of the skin preprocessed by mean centering, normalization followed by mean centering, and autoscaling. The models were constructed with four, three, and three latent variables for mean centering, normalization followed by mean centering, and autoscaling, respectively. All three models produced a total of four classification errors, and the misclassified samples for models with preprocessing of mean centering and normalization followed by mean centering were the same. Most of the samples were correctly classified according to their ripeness degree.

Discussion

During the ripening process of avocados, changes in color, flavor, and texture occur simultaneously. Changes in texture occur through the breakdown of cellulose and pectin into smaller water-soluble components due to the increased activity of cellulase and

pectinase (Paliyath et al. 2008). The skin color changes owing to the decrease in chlorophyll and increase in anthocyanins (Cox et al. 2004). Additionally, high polyphenol oxidase activity in the flesh leads to enzymatic browning (Paliyath et al. 2008). Prediction of the ripening degree by FF measurement aims to capture these simultaneous changes from the chemical viewpoint and create a link to the physical aspects, such as the hardness which is an important sensory quality for consumers.

Figure 3 shows the fluorescence intensity at some of the wavelengths that made large contributions to the PLS regression models, judging from their high VIP values. Fig. 3(a) shows the emission spectra of the skin at Ex 540 nm, corresponding to the large VIP peak in Fig. 2(f). Excluding the sharp peaks around Em 800 and 810 nm, which are related to Raman scattering, there is a general trend ranging from unripe (high fluorescence intensity) to overripe (low fluorescence intensity). To view this trend in more detail, the fluorescence intensity at Ex 540 nm and Em 780 nm was plotted against the fruit hardness value. This pair of wavelengths corresponds to the peak wavelength in Fig. 2(f). Although there is some variation among the samples with hardness values around 18 N cm^{-2}, the fluorescence intensity decreases as the hardness value decreases. This corresponds to the

literature stating that the chlorophyll content decreases as ripening progresses (Cox et al. 2004). The reason that some unripe samples showed low fluorescence values may be that the curved sample surface was not completely in contact with the measurement window.

Figure 3(c) shows the fluorescence intensity of avocado flesh measured at Ex 290 nm and Em 330 nm plotted against the hardness value of the fruit. The fluorescence intensities are shown as normalized values because the models used to obtain Fig. 2(a) and 2(d) were constructed from the normalized FFs. The fluorescence intensity gradually decreases as the hardness value decreases from 30 to 5 N cm^{-2} and then rapidly decreases as the hardness value approaches 0 N cm^{-2}.

This nonlinear relation with hardness suggested that better models could be created by converting hardness values to a log scale, because PLS is a linear model. However, converting hardness values to a log scale produced models with relatively large mean errors. This was because the RMSE is calculated after converting the predicted objective variables back to a linear scale, which magnifies the error when the values are large. Nonlinear prediction models such as the support vector machine (SVM) and kernel methods (Muller et al. 2001) may be suitable.

The fluorescence peak observed from the avocado flesh around the wavelengths shown in Fig. 3(c) can be attributed to many fluorescence constituents such as tryptophan, tocopherols, and several polyphenols such as epicatechin. However, we are unaware of any reports indicating the decrease in these constituents as ripening progresses. A possible hypothesis for this decrease in fluorescence intensity is the reabsorption of fluorescence or competition for excitation light with other chemical constituents that increase with ripening. A similar phenomenon is observed in apples and grapes, where the fluorescence intensity of chlorophyll decreases owing to the increase in anthocyanins, which compete with chlorophyll for the absorption of incident light (Agati et al. 2007; Merzlyak et al. 2008). The avocado flesh becomes dark with overripening owing to polyphenol oxidase activity (Kahn 1975; Zauberman and Jobin-Decor 1995), and the oxidized polyphenols absorb light.

The oxidation of avocado flesh and the resulting decrease in fluorescence were indicated by cutting a ripe avocado and measuring the fluorescence of the flesh over time (for 180 min at 30 min intervals). Figure 4 shows the change in fluorescence intensity at Ex 290 nm and Em 330 nm of several samples and images of the measured surface

acquired with a flat-bed scanner (GT-X980, Epson, Japan). Although the initial fluorescence intensity differed between samples, it followed a similar trend of decreasing with time. These data support the hypothesis that the decrease in intensity at these short wavelengths is not due to the decrease in some constituents with ripening, but rather due to the increase in oxidized components, which indirectly leads to the decrease in fluorescence intensity. Enzymatic activity in the avocado mesocarp has been studied in relation to flesh discoloration, and polyphenols such as epicatechin (George and Christoffersen 2016), caffeic acid, chlorogenic acid, and catechins (Van Lelyveld et al. 1984) are known to be oxidized by polyphenol oxidase.

For practical use, the discrimination of ripe fruits through measurement of the skin will be necessary. In this respect, the results obtained from the PLS discrimination analysis show the applicability of this technique for ensuring uniform products. Although the discrimination accuracy was relatively high, there were a few misclassifications and the characteristics of the misclassified fruits were investigated. In this study, we measured two points on the skin for the FF data, and the two sets of data were analyzed in the model as two samples. Therefore, the predicted groups may have been different for the two

measurements from the same sample. This was the case for all the misclassifications, except for the two ripe samples misclassified as unripe. This fruit showed a hardness value of 5.92 N cm^{-2}, which is on the borderline between ripe and unripe. Interestingly, all the other misclassified measurements were measured near the basal end. The larger curvature at the basal end may have induced changes in the reflectance, resulting in classification errors.

PLS regression and PLS-DA models have an potential of improvement through variable selection using indices such as VIP and Selectivity Ratio (SR) (Trivittayasil et al. 2018) and the discriminating variable (DIVA) test (Rajalahti et al. 2009). Effective variable selection eliminates uninformative and irrelevant variables and decreases the risk of overfitting (Goodarzi and dos Santos Coelho 2014), and also leads to shorter measuring time. The prediction models presented in this study could also be improved by variable selection, leading to quick and accurate measurement of ripeness.

Conclusions

FFs of the skin and flesh of avocados proved to contain useful information on the degree

of ripeness of the fruit. Although FFs of the flesh, only measurable by cutting the fruit, could predict the hardness value of avocados with higher accuracy, FFs of the skin captured the ripening process well. The degree of ripeness (unripe, ripe, and overripe) was predicted from the FFs of the skin with an accuracy of 90 % for the validation dataset, and misclassifications occurred for fruit on the borderline or for measurements near the basal end. By selecting fluorescence wavelength conditions that are important for the PLS models constructed in this study, quicker and more accurate monitoring may be possible, enabling the use of this technique in the distribution of agricultural products.

Acknowledgements

This work was supported by JSPS KAKENHI Grant Number JP17K15354.

Compliance with Ethical Standards:

Funding: This work was supported by JSPS KAKENHI Grant Number JP17K15354.

Conflict of interest: Mito Kokawa declares that she has no conflict of interest. Azusa Hashimoto declares that she has no conflict of interest. Xinyue Li declares that she has

no conflict of interest. Mizuki Tsuta declares that he has no conflict of interest. Yutaka Kitamura declares that he has no conflict of interest.

Ethical approval: This article does not contain any studies with human participants or animals performed by any of the authors.

Informed consent: Not applicable.

References

Agati G, Meyer S, Matteini P, Cerovic ZG (2007) Assessment of Anthocyanins in Grape (Vitis vinifera L.) Berries Using a Noninvasive Chlorophyll Fluorescence Method Journal of agricultural and food chemistry 55:1053-1061 doi:10.1021/jf062956k

Belay A, Kim HK, Hwang YH (2016) Binding of caffeine with caffeic acid and chlorogenic acid using fluorescence quenching, UV/vis and FTIR spectroscopic techniques Luminescence : the journal of biological and chemical luminescence 31:565-572 doi:10.1002/bio.2996

Chong I-G, Jun C-H (2005) Performance of some variable selection methods when multicollinearity is present Chemometrics and Intelligent Laboratory Systems 78:103-112 doi:https://doi.org/10.1016/j.chemolab.2004.12.011

Cox KA, McGhie TK, White A, Woolf AB (2004) Skin colour and pigment changes during ripening of 'Hass' avocado fruit Postharvest Biology and Technology 31:287-294 doi:https://doi.org/10.1016/j.postharvbio.2003.09.008

Fujita K, Tsuta M, Kokawa M, Sugiyama J (2010) Detection of deoxynivalenol using fluorescence excitation-emission matrix Food and Bioprocess Technology 3:922-927

Gaete-Garretón L, Vargas-Hernndez Y, León-Vidal C, Pettorino-Besnier A (2005) A Novel Noninvasive Ultrasonic Method to Assess Avocado Ripening Journal of Food Science 70:E187-E191 doi:10.1111/j.1365-2621.2005.tb07134.x

George HL, Christoffersen RE (2016) Differential latency toward (–)-epicatechin and

catechol mediated by avocado mesocarp polyphenol oxidase (PPO) Postharvest Biology and Technology 112:31-38 doi:https://doi.org/10.1016/j.postharvbio.2015.09.036

Goodarzi M, dos Santos Coelho L (2014) Firefly as a novel swarm intelligence variable selection method in spectroscopy Anal Chim Acta 852:20-27 doi:10.1016/j.aca.2014.09.045

Guimet F, Ferre J, Boque R, Rius FX (2004) Application of unfold principal component analysis and parallel factor analysis to the exploratory analysis of olive oils by means of excitation-emission matrix fluorescence spectroscopy Analytica Chimica Acta 515:75-85

Jiang JK, Wu J, Liu XH (2010) Fluorescence properties of lake water Spectroscopy and Spectral Analysis 30:1525-1529 doi:10.3964/j.issn.1000-0593(2010)06-1525-05

Kahn V (1975) Polyphenol oxidase activity and browning of three avocado varieties Journal of the Science of Food and Agriculture 26:1319-1324 doi:doi:10.1002/jsfa.2740260910

Kokawa M et al. (2015) Measuring cheese maturation with the fluorescence fingerprint Food Science and Technology Research 21:549-555

Kokawa M, Nishi K, Ashida H, Trivittayasil V, Sugiyama J, Tsuta M (2016) Predicting the Heating Temperature of Soymilk Products Using Fluorescence Fingerprints Food and Bioprocess Technology:1-7 doi:10.1007/s11947-016-1835-6

Landahl S, Meyer MD, Terry LA (2009) Spatial and Temporal Analysis of Textural and Biochemical Changes of Imported Avocado cv. Hass during Fruit Ripening Journal of agricultural and food chemistry 57:7039-7047 doi:10.1021/jf803669x

Lang M, Stober F, Lichtenthaler HK (1991) Fluorescence emission spectra of plant leaves and plant constituents Radiation and Environmental Biophysics 30:333-347 doi:10.1007/bf01210517

Lenhardt L, Bro R, Zeković I, Dramićanin T, Dramićanin MD (2015) Fluorescence spectroscopy coupled with PARAFAC and PLS DA for characterization and classification of honey Food Chemistry 175:284-291 doi:https://doi.org/10.1016/j.foodchem.2014.11.162

Lucas A, Andueza D, Rock E, Martin B (2008) Prediction of Dry Matter, Fat, pH, Vitamins, Minerals, Carotenoids, Total Antioxidant Capacity, and Color in Fresh and Freeze-Dried Cheeses by Visible-Near-Infrared Reflectance Spectroscopy Journal of agricultural and food chemistry 56:6801-6808 doi:10.1021/jf800615a

Magwaza LS, Tesfay SZ (2015) A Review of Destructive and Non-destructive Methods

for Determining Avocado Fruit Maturity Food and Bioprocess Technology 8:1995-2011 doi:10.1007/s11947-015-1568-y

Merzlyak MN, Melø TB, Naqvi KR (2008) Effect of anthocyanins, carotenoids, and flavonols on chlorophyll fluorescence excitation spectra in apple fruit: signature analysis, assessment, modelling, and relevance to photoprotection Journal of Experimental Botany 59:349-359 doi:10.1093/jxb/erm316

Moller JKS, Parolari G, Gabba L, Christensen J, Skibsted LH (2003) Monitoring chemical changes of dry-cured parma ham during processing by surface autofluorescence spectroscopy Journal of agricultural and food chemistry 51:1224-1230 doi:10.1021/jf025662h

Muller KR, Mika S, Ratsch G, Tsuda K, Scholkopf B (2001) An introduction to kernel-based learning algorithms Ieee Transactions on Neural Networks 12:181-201

Paliyath G, Murr DP, Handa AK, Lurie S (2008) Postharvest Biology and Technology of Fruits, Vegetables, and Flowers. Wiley-Blackwell Publishing, Iowa, USA

Pareek S (ed) (2016) Postharvest Ripening Physiology of Crops. Innovations in postharvest technology series. CRC Press, Florida, USA

Rajalahti T, Arneberg R, Kroksveen AC, Berle M, Myhr KM, Kvalheim OM (2009) Discriminating Variable Test and Selectivity Ratio Plot: Quantitative Tools for Interpretation and Variable (Biomarker) Selection in Complex Spectral or Chromatographic Profiles Analytical Chemistry 81:2581-2590 doi:10.1021/ac802514y

Rodriguez-Carpena JG, Morcuende D, Andrade MJ, Kylli P, Estevez M (2011) Avocado (Persea americana Mill.) phenolics, in vitro antioxidant and antimicrobial activities, and inhibition of lipid and protein oxidation in porcine patties Journal of agricultural and food chemistry 59:5625-5635 doi:10.1021/jf1048832

Saeys W, Mouazen AM, Ramon H (2005) Potential for Onsite and Online Analysis of Pig Manure using Visible and Near Infrared Reflectance Spectroscopy Biosystems Engineering 91:393-402 doi:https://doi.org/10.1016/j.biosystemseng.2005.05.001

Schroeder CA (1987) Fluorescence of Tissues in Avocado Fruit California Avocado Society Yearbook 71:257-258

Schulman SG (1985) Molecular luminescence spectroscopy methods and applications: Part 1. John Wiley & Sons, Inc., New York

Sikorska E, Glisuzynska-Swiglo A, Insinska-Rak M, Khmelinskii I, De Keukeleire D, Sikorski M (2008) Simultaneous analysis of riboflavin and aromatic amino acids in beer

using fluorescence and multivariate calibration methods Analytica Chimica Acta 613:207-217 doi:10.1016/j.aca.2008.02.063

Trivittayasil V, Kameya H, Shoji T, Tsuta M, Kokawa M, Sugiyama J (2017) Simultaneous estimation of scavenging capacities of peach extract for multiple reactive oxygen species by fluorescence fingerprint method Food Chemistry doi:http://doi.org/10.1016/j.foodchem.2017.04.011

Trivittayasil V et al. (2015) Fluorescence fingerprint as an instrumental assessment of the sensory quality of tomato juices Journal of the Science of Food and Agriculture 96:1167-1174 doi:10.1002/jsfa.7199

Trivittayasil V et al. (2018) Classification of 1-methylcyclopropene treated apples by fluorescence fingerprint using partial least squares discriminant analysis with stepwise selectivity ratio variable selection method Chemometrics and Intelligent Laboratory Systems doi:https://doi.org/10.1016/j.chemolab.2018.02.004

Van Lelyveld LJ, Gerrish C, Dixont RA (1984) Enzyme activities and polyphenols related to mesocarp discolouration of avocado fruit Phytochemistry 23:1531-1534 doi:https://doi.org/10.1016/S0031-9422(00)83433-0

Williams PC, Sobering DC (1993) Comparison of Commercial near Infrared Transmittance and Reflectance Instruments for Analysis of Whole Grains and Seeds Journal of Near Infrared Spectroscopy 1:25-32 doi:10.1255/jnirs.3

Zauberman G, Jobin-Decor MP (1995) Avocado (Persea americana Mill.) quality changes in response to low-temperature storage Postharvest Biology and Technology 5:235-243 doi:https://doi.org/10.1016/0925-5214(94)00027-P

Tables

Table 1 Ripeness degree of avocados

Ripeness	Hardness ($N\ cm^{-2}$)	Description
Unripe	>6	tough mouthfeel, green flesh, unripe odor
Ripe	2-6	soft mouthfeel, green to yellow flesh
Overripe	<2	very soft and squishy, dark or black flesh, deteriorated quality

Table 2. Results of the PLS regression analysis with different preprocessing methods and measurement positions. The conditions in bold letters show the models that performed well.

	Preprocessing		Position	Number of LVs	RMSEC	RMSECV	RMSEP	R^2C	R^2CV	R^2P	RPD
	X	Y									
All samples	mean centering	-	skin	3	4.11	4.72	3.84	0.71	0.62	0.65	1.87
	normalization + mean centering	-	skin	2	4.12	4.65	4.17	0.71	0.63	0.62	1.72
	autoscaling	-	skin	3	4.04	4.79	3.96	0.72	0.61	0.63	1.81
	mean centering	log10	skin	4	4.74	5.72	4.82	0.64	0.52	0.53	1.49
	normalization + mean centering	log10	skin	3	4.92	5.63	4.12	0.61	0.52	0.64	1.74
	autoscaling	log10	skin	4	5.35	6.47	4.68	0.56	0.45	0.55	1.54
	mean centering	-	flesh	3	3.77	4.13	3.89	0.76	0.71	0.61	1.84
	normalization + mean centering	**-**	**flesh**	**6**	**2.65**	**3.37**	**3.57**	**0.88**	**0.81**	**0.70**	**2.01**
	autoscaling	-	flesh	4	2.99	3.57	3.47	0.85	0.78	0.70	2.07
	mean centering	log10	flesh	2	6.36	6.92	6.13	0.52	0.48	0.42	1.17
	normalization + mean centering	log10	flesh	3	4.54	4.90	3.67	0.70	0.66	0.64	1.95
	autoscaling	log10	flesh	1	6.11	6.23	5.68	0.42	0.41	0.36	1.27
Samples with hardness < 15 N cm^{-2}	mean centering	-	skin	6	1.63	2.61	2.65	0.85	0.62	0.59	1.57
	normalization + mean centering	-	skin	2	2.18	2.47	2.35	0.73	0.65	0.68	1.77
	autoscaling	**-**	**skin**	**4**	**1.91**	**2.34**	**2.05**	**0.79**	**0.69**	**0.75**	**2.03**
	mean centering	log10	skin	2	2.66	2.94	3.39	0.61	0.53	0.42	1.22
	normalization + mean centering	log10	skin	2	2.52	2.71	2.62	0.66	0.61	0.64	1.59
	autoscaling	log10	skin	4	2.47	2.85	2.39	0.68	0.60	0.69	1.74
	mean centering	-	flesh	3	2.33	2.71	2.07	0.69	0.58	0.76	2.00
	normalization + mean centering	-	flesh	1	2.76	3.04	2.88	0.56	0.47	0.53	1.44
	autoscaling	**-**	**flesh**	**5**	**1.68**	**2.49**	**2.02**	**0.84**	**0.65**	**0.75**	**2.05**
	mean centering	log10	flesh	4	2.69	3.17	4.05	0.63	0.53	0.62	1.02
	normalization + mean centering	log10	flesh	5	2.22	2.71	2.22	0.72	0.61	0.70	1.87
	autoscaling	log10	flesh	4	2.79	3.46	3.02	0.63	0.50	0.73	1.38

Table 3 Validation dataset results for the PLS discrimination analysis using the FFs of the skin. The FFs were preprocessed by mean centering, normalization followed by mean centering, and autoscaling, but there was no difference in the number of misclassified samples.

		Actual group		
		Unripe	Ripe	Over ripe
Predicted group	Unripe	17	2	0
	Ripe	1	10	1
	Over ripe	0	0	9

Figure captions

Fig 1

Average FFs of the skin (top row) and flesh (bottom row) of the unripe (left), ripe (center), and overripe (right) avocados. The color axis indicates the fluorescence intensity (arbitrary units).

Fig 2

Regression plots (top row) and the variance of importance (VIP) plots (bottom row) of three models constructed to predict the hardness of the flesh from FF measurements. The left model ((a) and (d)) used the FFs of the flesh coupled with preprocessing by normalization followed by mean centering. The model shown in the center ((b) and (e)) were constructed from FFs of the flesh preprocessed by autoscaling, and samples with hardness values above 15 N cm^{-2} were removed. The model on the right ((c) and (f)) show the model constructed from FFs of the skin, preprocessed with autoscaling, where samples with hardness values above 15 N cm^{-2} were removed.

Fig 3

Fluorescence spectra and intensities at some of the wavelengths that made large

contributions to the PLS regression models. (a) shows the fluorescence spectra of the skin at Ex 540 nm. (b) shows the fluorescence intensity at Ex 540 nm and Em 780 nm plotted against the fruit hardness value. (c) shows the normalized fluorescence intensity of avocado flesh measured at Ex 290 nm and Em 330 nm plotted against the hardness value of the fruit.

Fig 4

The change in fluorescence intensity of the flesh at Ex 290 nm and Em 330 nm taken over time (a) and the corresponding images of the measured surface acquired with a flat-bed scanner (b).

Figure 1

Click here to access/download;Figure;Figure 1.tif

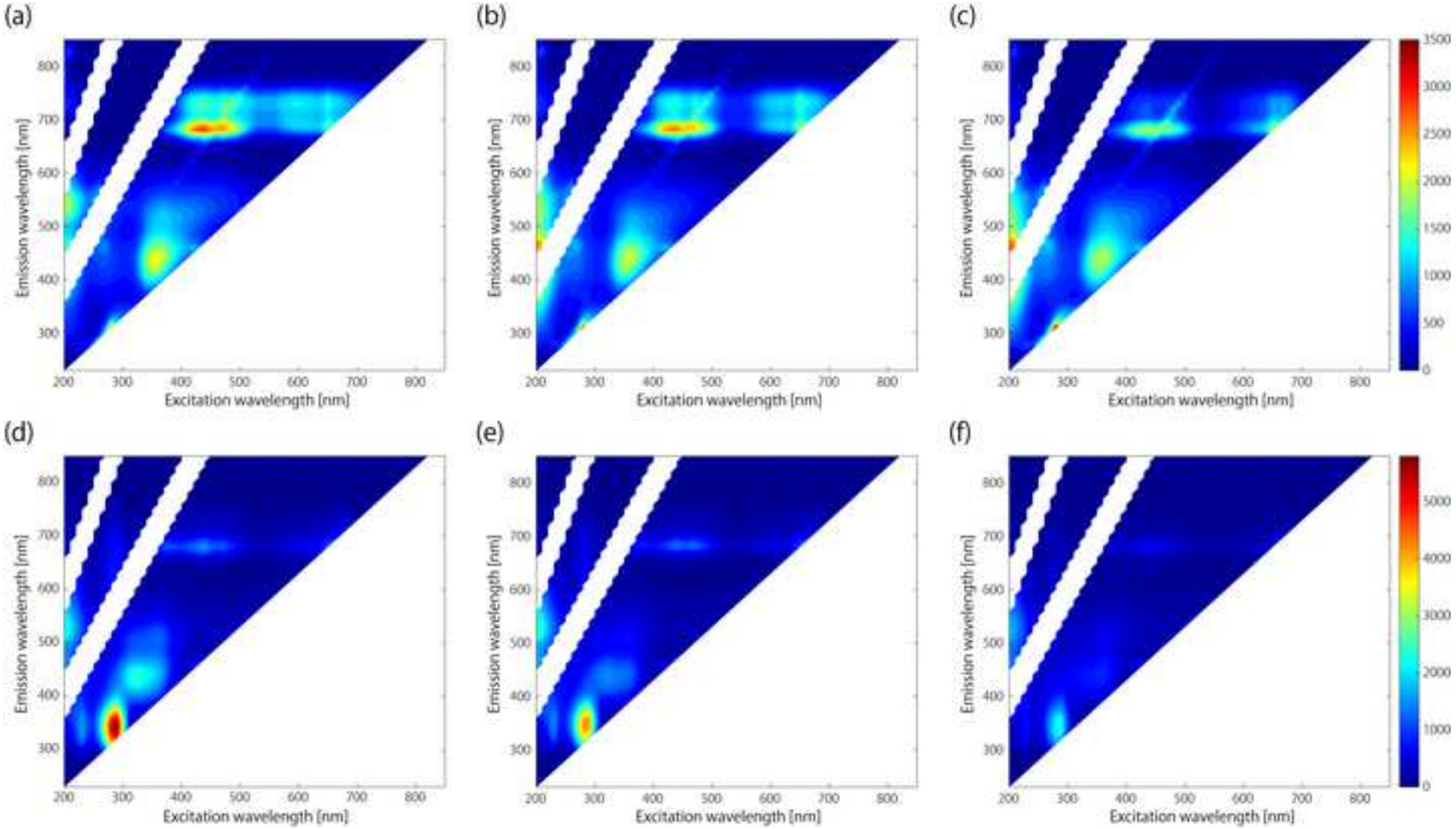

Figure 2

Click here to access/download;Figure;Figure 2.tif

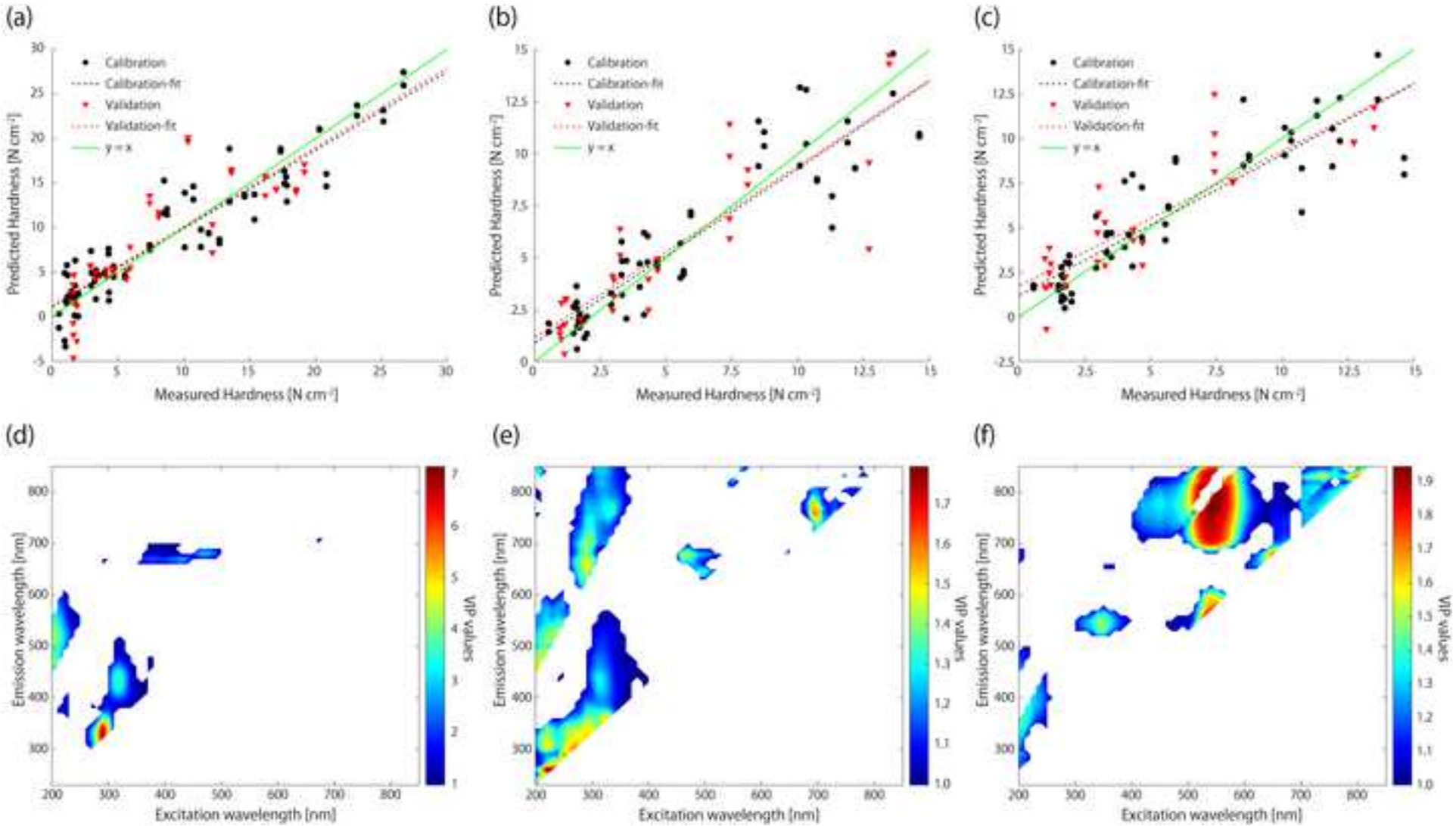

Figure 3

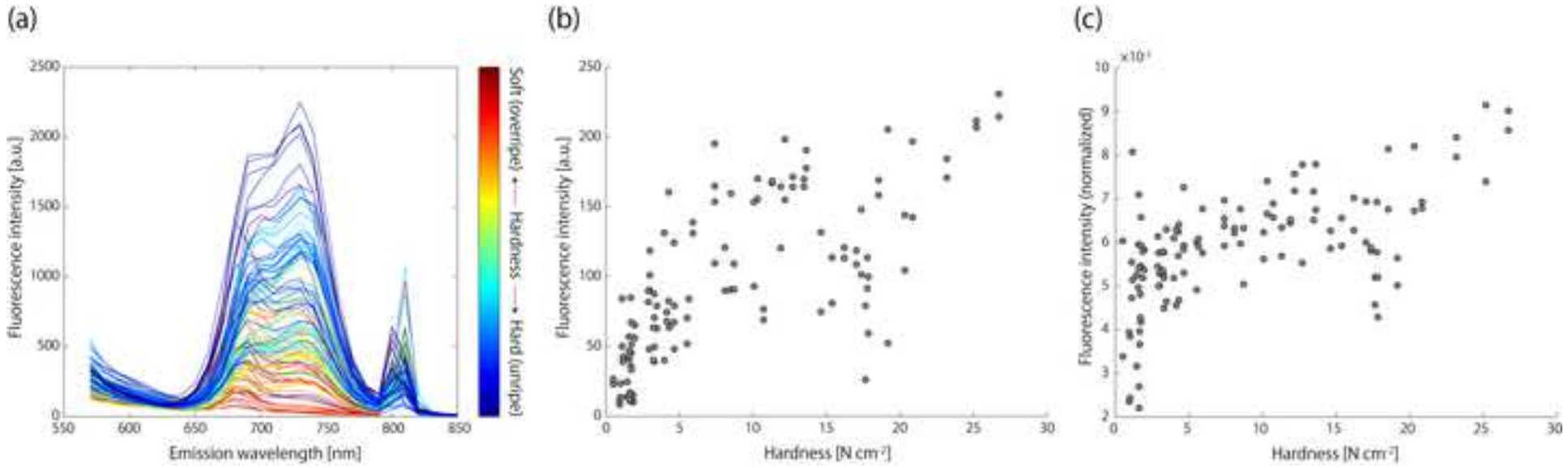

Figure 4